Electronic Supplementary Material (ESI) for ChemComm.

Tetrabenzanthanthrenes by mitigation of rearrangements in the planarization of *ortho*-phenylene hexamers

Supporting Information

*Jian He, Sanyo Mathew, Zacharias J. Kinney, Rachel M. Warrell, James S. Molina, C. Scott Hartley**

Department of Chemistry & Biochemistry, Miami University, Oxford, OH 45056, USA

Table of Contents

List of Figures

List of Schemes

List of Tables

Formation of TBAA′

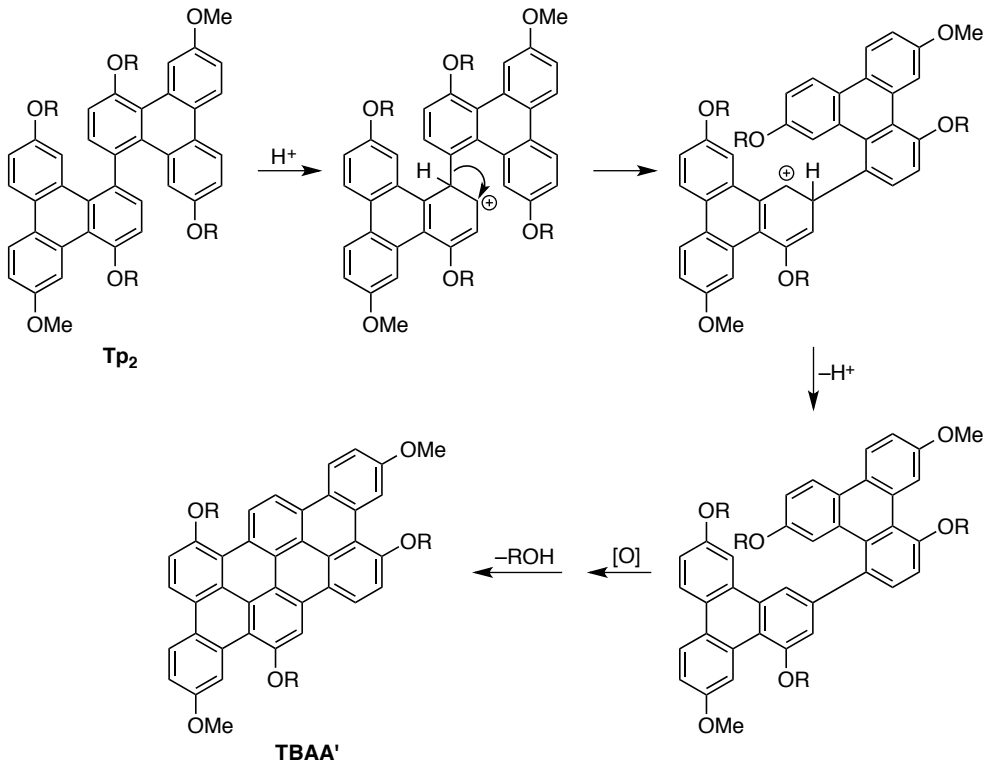

Scheme S1. Rearrangement mechanism leading to the formation of **TBAA′**.

Geometry of TBAA

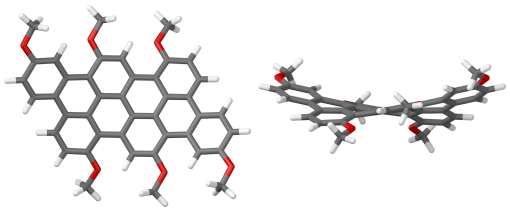

Figure S1. Optimized geometry (B3LYP/6-31+G(d,p)) of **TBAA**. The side chains have been simplifed to methoxy groups. This C_2 symmetric) conformer is favored over the C_i symmetric conformer by 0.5 kcal/mol.

Characterization of TBAA′

To confirm the structure of the rearranged product **TBAA′**, the ^{1}H and ^{13}C NMR chemical shifts were fully assigned using a combination of COSY (Figure S22), HMQC (Figure S23), and HMBC (Figure S24) spectra in chloroform-*d*. The isotropic shieldings for the aromatic protons and carbons were then calculated using the GIAO method at the PCM/WC04/6-31G(d)//B3LYP/6-31G(d) level, using a simplified version of the proposed geometry (all alkoxy groups truncated at methoxy). The alkoxy groups were oriented according to a conformational search at the PM6 level.

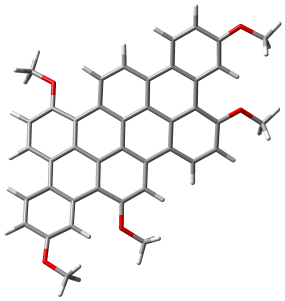

Figure S2. Optimized geometry (B3LYP/6-31G(d)) of **TBAA′**. $E = -1955.410140\ E_h$, 0 imaginary frequencies.

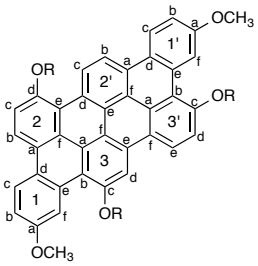

Figure S3. NMR assignment labelling for **TBAA′**. R = 3,5-dimethyloctyl.

Position	^{1}H δ	^{13}C δ	^{13}C IS
1a		157.5	49.04
1b	7.66	116.1	87.21
1c	8.61	124.0	77.69
1d		124.6	80.11
1e		129.8	71.12
1f	9.28	111.5	94.98
2a		123.9	79.40
2b	8.70	120.9	81.60
2c	7.66	113.0	93.72
2d		156.9	51.13
2e		119.4	83.37
2f		127.6	75.31
3a		n/d	72.84
3b		117.2	86.96
3c		155.9	48.74
3d	8.44	105.1	100.89
3e		n/d	72.09
3f		n/d	85.81
1′a		158.2	47.91
1′b	7.36	115.9	87.28
1′c	8.86	124.8	76.97
1′d		124.8	80.54
1′e		131.2	69.43
1′f	9.41	111.7	95.23
2′a		127.9	73.73
2′b	8.92	118.3	86.43
2′c	10.18	127.4	74.58
2′d		n/d	78.40
2′e		125.0	76.06
2′f		n/d	82.37
3′a		n/d	71.66
3′b		118.1	85.77
3′c		155.3	47.60
3′d	7.54	111.5	95.93
3′e	8.70	120.9	77.36
3′f		122.6	82.06

Table S1. Experimental chemical shift assignments and calculated ^{13}C isotropic shieldings for **TBAA′**.

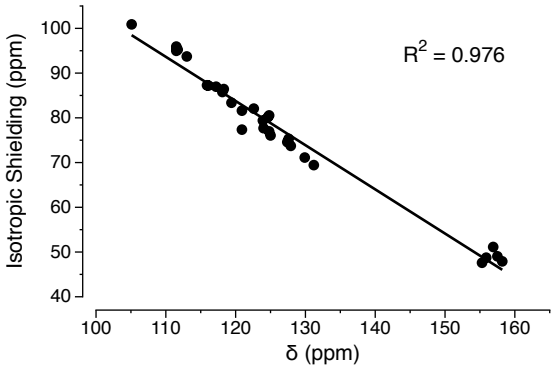

Figure S4. Calculated isotropic shieldings (PCM/WP04/6-31G(d)) vs experimental δ for **TBAA′**.

Complete Computational Results

All calculations of the reaction mechanisms were performed at the PCM(dichloromethane)/B3LYP/6-31+G(d,p) level using Gaussian 09.[1] The nature of all stationary points was confirmed through frequency analysis, which gave 0 or 1 imaginary frequencies for energy minima or transition states, respectively. For the calculations on radical cations, $\langle S^2 \rangle$ differed from the ideal value of 0.75 by <10% in all cases[2] and wavefunction stability was verified. Values of G° are reported at 298.150 K. Scaling factors were not applied to the thermochemistry. Cartesian coordinates for all computational geometries are included in a separate plain text Supporting Information file.

Comparison with literature data

Some of the calculations on *o*-terphenyl (**Bp-Ph**) have direct comparisons in the literature. For example, our calculated barrier for the rearrangement of **Bp-Ph** to *m*-terphenyl is 14.6 kcal/mol, an excellent match to Johnson's value of 14.7 kcal/mol calculated at the same level of theory[3] (the small difference likely results from our use of dichloromethane as the solvent rather than dichloroethane). The calculations on planarization of **Bp-Ph** by the arenium cation mechanism are not directly comparable to King's (we have used a larger basis set and solvent is handled differently); however, the results are similar (our barrier and endergonicity are 5 kcal/mol higher).[4] Finally, the barrier ($\Delta G^\ddagger$ = 26 kcal/mol) and endergonicity (ΔG° = 23 kcal/mol) of planarization of **Bp-Ph** by the radical cation mechanism are in good agreement with the results of Di Stefano and Negri ($\Delta H^\ddagger$ = 22 kcal/mol and ΔH° = 20 kcal/mol).[5]

Reference Acid and Oxidant

Structure		E (E_h)	ZPC (E_h)	G° (E_h)	IF
C_6H_6	D_{6h}	−232.270732	0.100352	−232.195513	0
$C_6H_7^+$	C_{2v}	−232.560619	0.110460	−232.561267	0
$C_6H_6^{\cdot +}$	C_{2h}	−232.008973	0.097821	−231.939263	0

Table S2. Computational data for benzene, protonated benzene, and benzene radical cation. E is the energy, ZPC is the zero-point correction, and IF is the number of imaginary frequencies.

1,2-Rearrangement

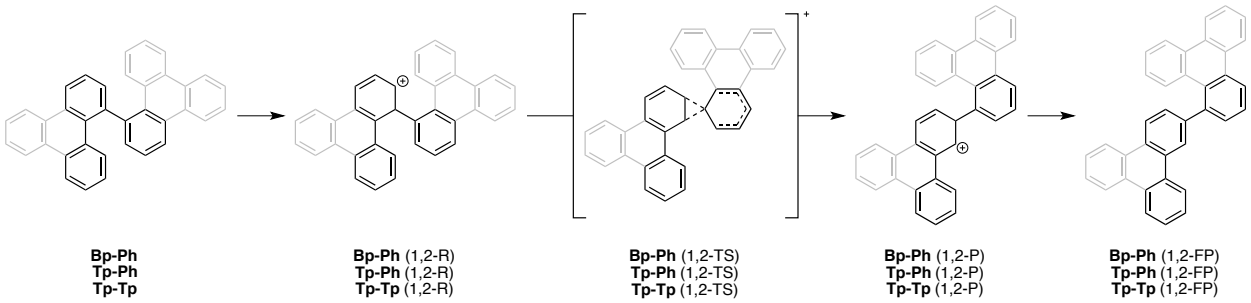

Scheme S2. 1,2-Rearrangement by *ipso* protonation.

Structure		E (E_h)	ZPC (E_h)	G° (E_h)	IF
Bp-Ph	C_2	−694.408227	0.261759	−694.187287	0
Bp-Ph (1,2-R)	C_1	−694.783327	0.273553	−694.552170	0
Bp-Ph (1,2-TS)	C_1	−694.760830	0.272733	−694.528835	1
Bp-Ph (1,2-P)	C_1	−694.775015	0.272581	−694.545234	0
Bp-Ph (1,2-FP)	C_s	−694.414637	0.262065	−694.194133	0
Tp-Ph	C_1	−924.284915	0.321685	−924.008353	0
Tp-Ph (1,2-R)	C_1	−924.671177	0.333356	−924.384108	0
Tp-Ph (1,2-TS)	C_1	−924.652357	0.332733	−924.364567	1
Tp-Ph (1,2-P)	C_1	−924.672507	0.333323	−924.386402	0
Tp-Ph (1,2-FP)	C_1	−924.299474	0.321876	−924.023372	0
Tp-Tp	C_2	−1385.229506	0.462132	−1384.822415	0
Tp-Tp (1,2-R)	C_1	−1385.610204	0.474118	−1385.191503	0
Tp-Tp (1,2-TS)	C_1	−1385.590503	0.473559	−1385.173268	1
Tp-Tp (1,2-P)	C_1	−1385.612840	0.473524	−1385.196410	0
Tp-Tp (1,2-FP)	C_1	−1385.241602	0.462174	−1384.835703	0

Table S3. Computational data for structures related to 1,2-rearrangement. E is the energy, ZPC is the zero-point correction, and IF is the number of imaginary frequencies.

Planarization: Arenium Cation Mechanism

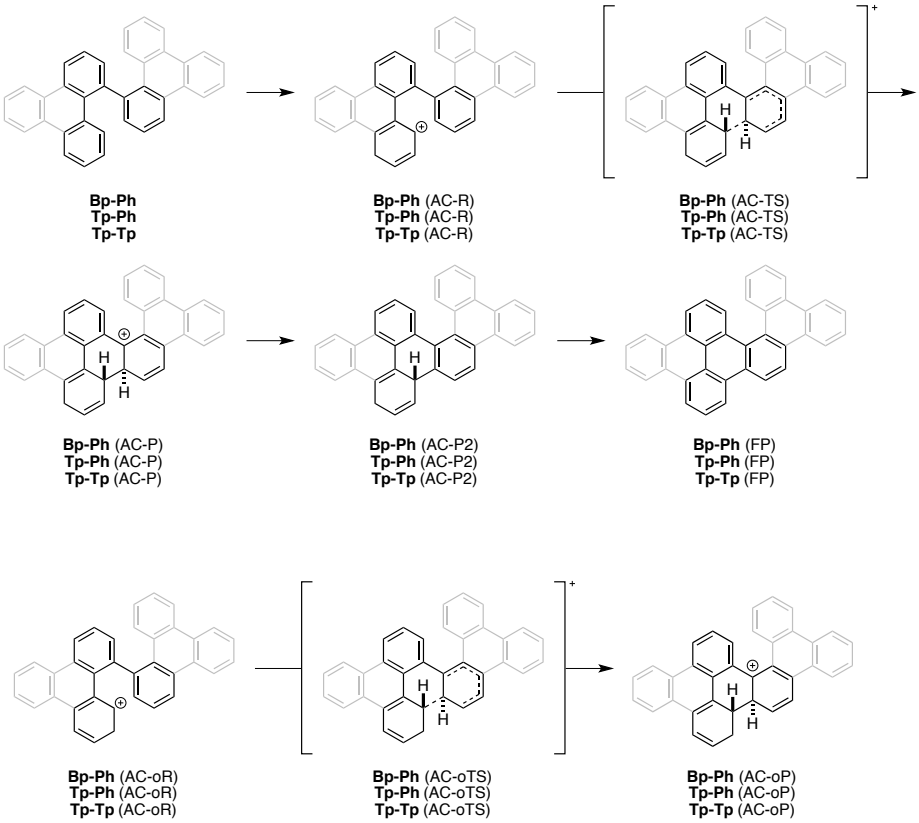

Scheme S3. Arenium cation planarization.

Structure		E (E_h)	ZPC (E_h)	$G°$ (E_h)	IF
Bp-Ph	C_2	−694.408227	0.261759	−694.187287	0
Bp-Ph (AC-R)	C_1	−694.782185	0.271858	−694.552440	0
Bp-Ph (AC-TS)	C_1	−694.757264	0.273318	−694.523172	1
Bp-Ph (AC-P)	C_1	−694.764744	0.274326	−694.530272	0
Bp-Ph (AC-P2)	C_1	−694.383172	0.262926	−694.159283	0
Bp-Ph (FP)	C_{2v}	−693.227249	0.241079	−693.024705	0
Bp-Ph (AC-oR)	C_1	−694.781802	0.272096	−694.551421	0
Bp-Ph (AC-oTS)	C_1	−694.754381	0.273334	−694.520212	1
Bp-Ph (AC-oP)	C_1	−694.770060	0.274641	−694.535210	0
Tp-Ph	C_1	−924.284915	0.321685	−924.008353	0
Tp-Ph (AC-R)	C_1	−924.673321	0.332522	−924.386484	0
Tp-Ph (AC-TS)	C_1	−924.647945	0.333128	−924.358061	1
Tp-Ph (AC-P)	C_1	−924.659198	0.334466	−924.368522	0
Tp-Ph (AC-P2)	C_1	−924.274684	0.322923	−923.994776	0
Tp-Ph (FP)	D_{2h}	−923.114482	0.300393	−922.856412	0
Tp-Ph (AC-oR)	C_1	−924.671722	0.332295	−924.385449	0
Tp-Ph (AC-oTS)	C_1	−924.641356	0.333010	−924.351541	1
Tp-Ph (AC-oP)	C_1	−924.666915	0.334620	−924.375856	0
Tp-Tp	C_2	−1385.229506	0.462132	−1384.822415	0
Tp-Tp (AC-R)	C_1	−1385.617212	0.473030	−1385.200085	0
Tp-Tp (AC-TS)	C_1	−1385.594143	0.473501	−1385.174020	1
Tp-Tp (AC-P)	C_1	−1385.607517	0.475122	−1385.185843	0
Tp-Tp (AC-P2)	C_1	−1385.203752	0.462999	−1384.794136	0
Tp-Tp (FP)	C_1	−1384.050077	0.440868	−1383.661666	0
Tp-Tp (AC-oR)	C_1	−1385.615674	0.472798	−1385.199044	0
Tp-Tp (AC-oTS)	C_1	−1385.587771	0.473359	−1385.168076	1
Tp-Tp (AC-oP)	C_1	−1385.615150	0.475163	−1385.193319	0

Table S4. Computational data for structures related to arenium cation planarization. E is the energy, ZPC is the zero-point correction, and IF is the number of imaginary frequencies.

Planarization: Radical Cation Mechanism

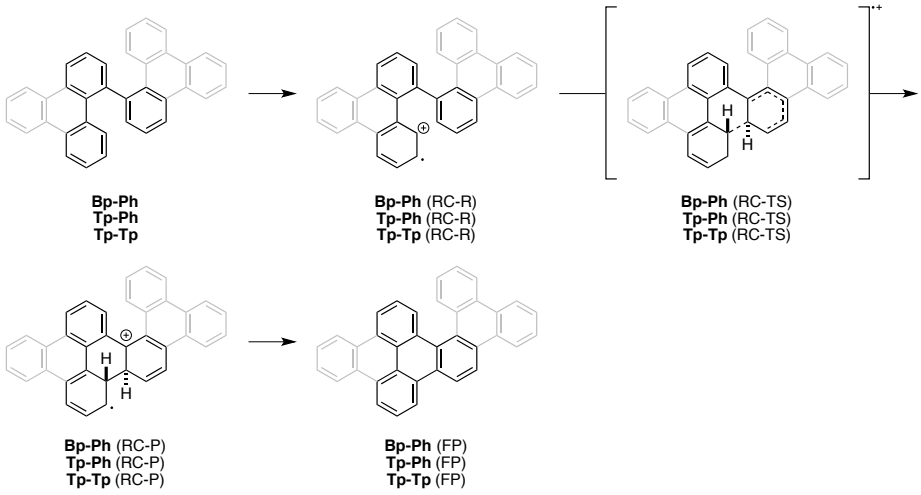

Scheme S4. Radical cation planarization.

Structure		E (E_h)	ZPC (E_h)	$G°$ (E_h)	IF
Bp-Ph	C_2	−694.408227	0.261759	−694.187287	0
Bp-Ph (RC-R)	C_2	−694.183349	0.261758	−693.962511	0
Bp-Ph (RC-TS)	C_1	−694.141326	0.259803	−693.920613[a]	1
Bp-Ph (RC-P)	C_2	−694.148020	0.262016	−693.925960	0
Bp-Ph (FP)	C_{2v}	−693.227249	0.241079	−693.024705	0
Tp-Ph	C_1	−924.284915	0.321685	−924.008353	0
Tp-Ph (RC-R)	C_1	−924.066254	0.321275	−923.790528	0
Tp-Ph (RC-TS)	C_1	−924.028888	0.319635	−923.753084	1
Tp-Ph (RC-P)	C_1	−924.036474	0.321365	−923.760062	0
Tp-Ph (FP)	D_{2h}	−923.114482	0.300393	−922.856412	0
Tp-Tp	C_2	−1385.229506	0.462132	−1384.822415	0
Tp-Tp (RC-R)	C_2	−1385.015570	0.461682	−1384.608850	0
Tp-Tp (RC-TS)	C_1	−1384.977477	0.460851	−1384.570505	1
Tp-Tp (RC-P)	C_1	−1384.982321	0.461999	−1384.574063	0
Tp-Tp (FP)	C_1	−1384.050077	0.440868	−1383.661666	0

Table S5. Computational data for structures related to radical cation planarization. E is the energy, ZPC is the zero-point correction, and IF is the number of imaginary frequencies. [a]We were unable to locate a TS with strict C_2 symmetry. The free energy has been corrected by $RT\,ln2$ to account for this.

Photophysical Properties of TBAA and Tp_2

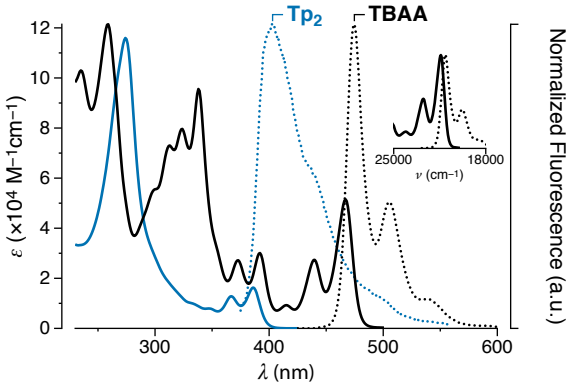

Figure S5. UV/Vis and fluorescence spectra of **TBAA** and $\mathbf{Tp_2}$ in CH_2Cl_2.

Compound	Stokes Shift (nm)	Φ	τ (ns)	k_r (ns^{-1})	k_{nr} (ns^{-1})
TBAA	8	0.51	4.2	0.12	0.12
$\mathbf{Tp_2}$	16	0.30	2.9	0.10	0.24

Table S6. Photophysical properties of compounds **TBAA** and $\mathbf{Tp_2}$ in CH_2Cl_2.

Solution-Phase Aggregation of TBAA

^{1}H NMR spectra of **TBAA** were recorded at room temperature in $CDCl_3$ diluting from 6 mM to 0.3 mM. The chemical shifts of the aromatic protons were fit to eq 1:[6]

$$\delta = \Delta\delta\left(1 + \frac{1 - \sqrt{8K_dC + 1}}{4K_dC}\right) + \delta_m \tag{1}$$

The fit was performed using a custom Python 3 script (below). While it is not possible to distinguish dimerization

from isodesmic indefinite association using this model, the relatively small changes in chemical shift on going from monomer to aggregate ($\Delta\delta \approx 0.5$ ppm) suggest that association largely stops at the dimer.[6,7]

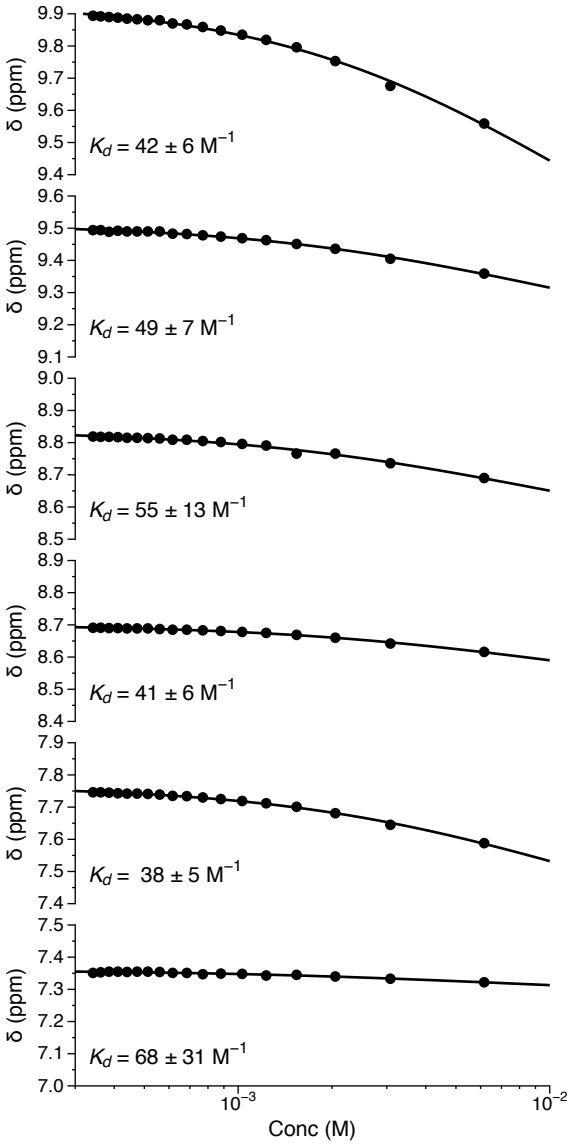

Figure S6. ^{1}H NMR chemical shift vs concentration for the aromatic protons of **TBAA** in chloroform-*d*. The lines are nonlinear least-squares fits to eq 1.

Python script used for curve fitting of NMR dilution experiments

Current versions of this script are hosted on GitHub.[8]

```
""" A simple python script that uses the leastsq function from SciPy to carry out a nonlinear
regression. Outputs a bunch of different measures to be used in judging the fit. Requires an input
file with x and y columns, no headings. Pass filename as an argument.


"""
import numpy, sys
from scipy.optimize import leastsq
```

```
# Define the function here, using p as an array of parameters. Functions must be able to take arrays
# as arguments (use numpy version of exp, for example).
def func(p, x):
    return (p[0] - p[1])*(1+(1-numpy.sqrt(8*p[2]*x+1))/(4*p[2]*x)) + p[1]

# Initial guesses for the parameters.
p0 = [10, 5, 600] # Pd Pm Ke


datafile = open(sys.argv[1])
x, y = numpy.array([]), numpy.array([])
for line in datafile:
    curline = line.replace("\n", "").split() # Splits at any whitespace.
    x = numpy.append(x, float(curline[0]))
    y = numpy.append(y, float(curline[1]))

# Defines the error function for leastsq. In for regression, it is just the residuals.
def func_res(p, x, y):
    return y - func(p, x)

dof = len(x) - len(p0) # Degrees of freedom

fit_parameters, covariance_matrix, info, msg, success \
    = leastsq(func_res, p0, args=(x,y), full_output=True)

sum_squares_residuals = sum(info["fvec"]*info["fvec"])
sum_squares_mean_dev = sum((y - numpy.mean(y))**2)

# The errors for each parameter are obtained by multiplying the covariance matrix by the residual
# variance (= sum_squares_residuals / dof).
errors = []
for i in range(len(covariance_matrix)):
    errors.append(numpy.sqrt(covariance_matrix[i,i]*sum_squares_residuals/dof))

print("**Regression results for file \"{}\"**".format(sys.argv[1]))
print()

print("Data (x, y, yfit)")
print("=================")
for n in range(len(x)):
    print("{}, {}, {}".format(x[n], y[n], y[n] + info["fvec"][n]))
print()

print("Optimized parameters")
print("====================")
for n in range(len(fit_parameters)):
    print("{} +/- {}".format(fit_parameters[n], errors[n]))
print()

print("Regression data")
```

```
print("===============")

# See leastsq documentation for descriptions of flags.
print("Flag: {}".format(success))

print("Std Deviation of residuals: {}".format(numpy.sqrt(sum_squares_residuals/dof)))
print("chi2 (sum square residuals): {}".format(sum_squares_residuals))

# Ideally, (reduced chi2)/(std dev of measurement) = 1.
print("Reduced chi2 (chi2/dof): {}".format(sum_squares_residuals/dof))
print("R2 = {}".format(1 - sum_squares_residuals/sum_squares_mean_dev))
print("Adjusted R2 = {}".format(1 - (sum_squares_residuals/dof)/(sum_squares_mean_dev/(len(x)-1))))
print("Covariance matrix:")
print(covariance_matrix*sum_squares_residuals/dof)
print("Residuals:")
print(info["fvec"])
```

Experimental

General

Unless otherwise noted, all starting materials, reagents, and solvents were purchased from commercial sources and used without further purification. Anhydrous THF was obtained by distillation from sodium/benzophenone. Anhydrous CH_2Cl_2 was obtained by distillation from CaH_2. Melting points were determined using a Thermal Analysis Q20 differential scanning calorimeter at a heating rate of 10 ℃/min. NMR spectra were measured for $CDCl_3$ solutions using Bruker Avance 300 or 500 MHz NMR spectrometers. Chemical shifts are reported in δ (ppm) relative to TMS, with the residual solvent protons used as internal standards ($CDCl_3$: 7.26 for ^{1}H, 77.16 for ^{13}C). High resolution ESI mass spectra were obtained from the Ohio State Mass Spectrometry and Proteomics Facility. High resolution MALDI mass spectra were obtained from the University of Akron Mass Spectrometry Center. UV–vis and fluorescence spectroscopy were performed using spectrometric-grade dichloromethane used without further purification. Fluorescence quantum yield and lifetime measurements were performed on solutions that had been sparged with nitrogen. Quantum yields were determined by reference to 9,10-diphenylanthracene in cyclohexane (Φ = 0.91) which was cross-checked with quinine bisulfate in 0.5 M H_2SO_4(aq) (Φ = 0.54). Five solutions of varying concentration were prepared for each sample and good fits ($R^2 \geq 0.99$) were obtained in all cases. The absorbance of all sample solutions was kept below 0.10 to avoid the inner-filter effect. Measurements were performed at room temperature with both sample and standard excited at the same wavelength. Fluorescence lifetimes were determined by time-correlated single-photon counting.

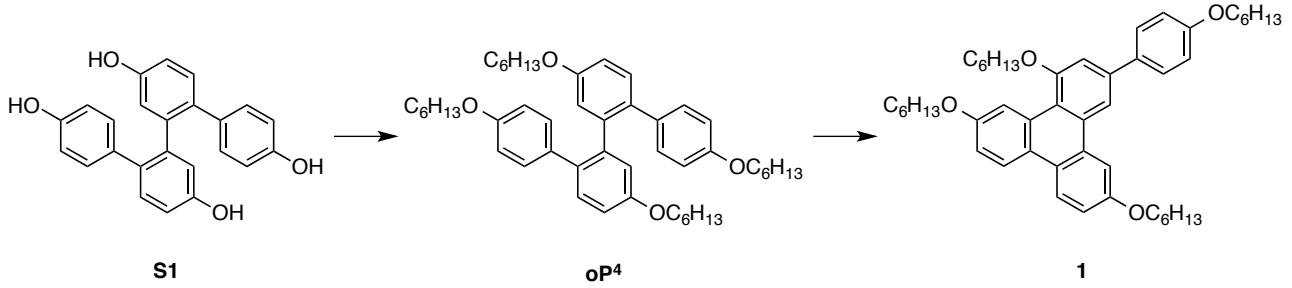

Scheme S5. Synthesis of compound **1**.

*Synthesis of **1***

***ortho*-Phenylene oP^4**

To a solution of *o*-phenylene **S1**[9] (200 mg, 0.540 mmol) in anhydrous DMF (15 mL) was added 1-bromohexane (0.61 mL, 4.3 mmol), K_2CO_3 (598 mg, 4.33 mmol), and KI (18 mg, 0.11 mmol). The mixture was stirred at 80–120

℃ for 2 d then cooled to rt. The mixture was diluted with EtOAc then acidified with 1 M HCl(aq). The aqueous layer was extracted with EtOAc, the the combined organic layers washed with water, dried ($MgSO_4$), filtered, and concentrated. Recrystallization ($EtOH/CH_2Cl_2$) gave compound **oP^4** (165 mg, 0.233 mmol, 43%) as a white solid: mp 106 ℃; ^{1}H NMR ($CDCl_3$, 500 MHz, Figure S7) δ 7.04 (d, $\mathcal{J}$ = 8.5 Hz, 2H), 6.93 (d, $\mathcal{J}$ = 2.6 Hz, 2H), 6.84 (dd, $\mathcal{J}$ = 8.5, 2.7 Hz, 2H), 6.6–6.5 (m, 8H), 4.0–3.8 (m, 8H), 1.8–1.7 (m, 8H), 1.5–1.4 (m, 8H), 1.4–1.3 (m, 16H), 1.0–0.9 (m, 12H); ^{13}C NMR ($CDCl_3$, 125 MHz, Figure S8) δ 157.9, 157.4, 141.2, 133.5, 133.4, 131.0, 130.2, 117.2, 114.0, 113.7, 68.3, 68.2, 31.8, 29.4, 25.91, 25.89, 22.8, 14.2; HRMS (ESI) calcd for $C_{48}H_{66}NaO_4$ ($M + Na^+$) 729.4859, found 729.4867.

Partially planarized *ortho*-phenylene 1

Compound **oP^4** (8.1 mg, 0.011 mmol) was dissolved in anhydrous CH_2Cl_2 (8 mL) and sparged with Ar for 15 min. A solution of $FeCl_3$ (13 mg, 0.08 mmol) in CH_3NO_2 (0.08 ml) was added dropwise. A stream of Ar was bubbled through the mixture throughout the reaction. The reaction was stirred for 30 min and then quenched with CH_3OH. The mixture was concentrated, then diluted with CH_2Cl_2, filtered through Celite, and concentrated. The crude product was purified by flash chromatography (5:2 hexanes:CH_2Cl_2) to give compound **1** (3.2 mg, 0.0045 mmol, 41%) as an amorphous white solid: ^{1}H NMR ($CDCl_3$, 500 MHz, Figure S9) δ 8.47 (d, $\mathcal{J}$ = 9.1 Hz, 1H), 8.43 (d, $\mathcal{J}$ = 8.9 Hz, 1H), 8.43 (s, 1H), 8.0–7.9 (m, 3H), 7.65 (d, $\mathcal{J}$ = 8.5 Hz, 2H), 7.25 (dd[a], 1H), 7.19 (dd, $\mathcal{J}$ = 8.9 Hz, 2.2 Hz, 1H), 7.02 (d, $\mathcal{J}$ = 8.5 Hz, 2H), 4.20 (t, $\mathcal{J}$ = 5.9 Hz, 2H), 4.19 (t, $\mathcal{J}$ = 6.0 Hz, 2H), 4.14 (t, $\mathcal{J}$ = 6.6 Hz, 2H), 4.05 (t, $\mathcal{J}$ = 6.5 Hz, 2H), 1.9–1.8 (m, 8H), 1.6–1.4 (m, 8H), 1.4–1.3 (m, 16H), 1.0–0.8 (m, 12H); ^{13}C NMR ($CDCl_3$, 125 MHz, Figure S10) δ 158.6, 158.0, 157.7, 155.9, 131.4, 131.1, 130.9, 130.4, 130.3, 130.0, 128.7, 125.9, 124.5, 124.39, 124.38, 124.0, 123.2, 115.4, 114.2, 107.7, 106.4, 105.4, 68.8, 68.5, 68.4, 68.2, 31.85, 31.81, 31.79, 31.7, 29.9, 29.62, 29.58, 29.5, 29.4, 26.02, 25.97, 25.9, 22.8, 14.21, 14.18; HRMS (ESI) calcd for $C_{48}H_{64}NaO_4$ ($M + Na^+$) 727.4702, found 727.4702.

*Synthesis of **TBAA***

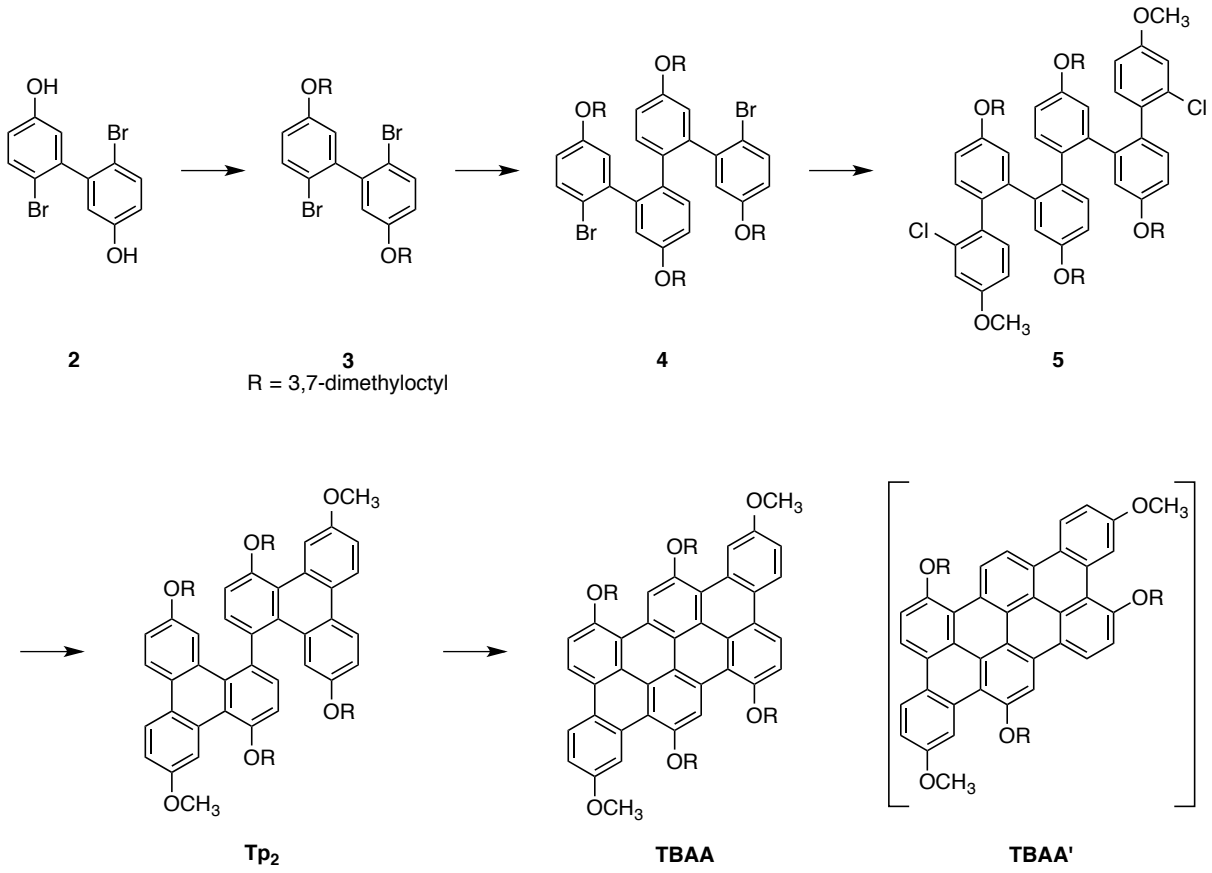

Scheme S6. Synthesis of compound **TBAA**.

[a] $\mathcal{J}$s could not be determined because of overlap with the $CHCl_3$ signal.

2,2'-Dibromo-5,5'-bis(3,7-dimethyloctyloxy)biphenyl (3)

A Schlenk vacuum tube was charged with 2,2'-dibromo-5,5'-dihydroxybiphenyl[10] **2** (3.44 g, 10.0 mmol), 1-bromo-3,7-dimethyloctane (8.85 g, 40.0 mmol), anhydrous K_2CO_3 (5.50 g, 39.8 mmol), and KI (160 mg, 0.96 mmol), then evacuated and backfilled with argon (3×). Anhydrous DMF (100 mL) was added and the Schlenk tube was sealed and heated at 90 ℃ for 2 d. The mixture was allowed to cool to rt, diluted with Et_2O, and poured into water. The organic layer was separated and the aqueous layer was extracted with Et_2O (5×). The combined organic layers were then washed with brine, dried ($MgSO_4$), filtered, and concentrated. Purification by flash chromatography (20:1 hexanes:EtOAc) gave compound **3** (5.36 g, <86%) as a sticky oil that contains a small amount of excess 1-bromo-3,7-dimethyloctane: ^{1}H NMR ($CDCl_3$, 500 MHz, Figure S11) δ 7.52 (d, $\mathcal{J}$ = 8.3 Hz, 2H), 6.9–6.8 (m, 4H), 4.0–3.9 (m, 4H), 1.9–1.0 (m, 20H), 0.95 (d, $\mathcal{J}$ = 6.5 Hz, 6H), 0.87 (d, $\mathcal{J}$ = 6.6 Hz, 12H); ^{13}C NMR ($CDCl_3$, 125 MHz, Figure S12) δ 158.3, 142.9, 133.2, 117.0, 116.1, 113.7, 66.8, 39.4, 37.4, 36.3, 30.0, 28.1, 24.8, 22.9, 22.81, 22.75, 19.8, 14.3; HRMS (ESI) calcd for $C_{32}H_{48}Br_2NaO_2$ ($M + Na^+$) 647.1896, found 647.1906.

***o*-Phenylene tetramer 4**

Under an inert atmosphere, a 1.6 M solution of *n*-BuLi in hexane (6.2 mL, 10 mmol) was added dropwise to a −78 ℃ solution of **3** (6.24 g, 10.0 mmol) in anydrous THF (170 mL). After 30 min, CuCN (465 mg, 5.20 mmol) was added in one portion. The reaction mixture was allowed to warm to rt and stirred for 2 h, then treated with duroquinone (2.50 g, 15.2 mmol). The mixture was stirred at rt for another 1.5 h, poured into 10% NH_3(aq) (300 mL), extracted with EtOAc (5×). The combined organic layers were washed with saturated NH_4Cl(aq) and water, dried ($MgSO_4$), filtered, and concentrated. The crude product was purified by flash chromatography (15:1 hexanes:EtOAc) to afford 3.32 g (61%) of compound **4** as a colorless sticky oil: ^{1}H NMR ($CDCl_3$, 500 MHz, Figure S13) the spectrum is broadened by slow conformational exchange, as would be expected for an *o*-phenylene tetramer with two terminal substituents[11] δ 7.6–6.4 (br, 12H), 4.0–3.6 (br, 8H), 1.9–0.9 (br, 76H); ^{13}C NMR ($CDCl_3$, 125 MHz, Figure S14) also complicated by slow conformational exchange; HRMS (ESI) calcd for $C_{64}H_{96}Br_2NaO_4$ ($M + Na^+$) 1111.5557, found 1111.5576.

***o*-Phenylene hexamer 5**

A Schlenk vacuum tube was charged with compound **4** (545 mg, 0.500 mmol), 2-chloro-4-methoxyphenylboronic acid (466 mg, 2.50 mmol), and $Pd(PPh_3)_4$ (35 mg, 0.030 mmol), then evacuated and backfilled with argon (3×). Degassed toluene (4.0 mL), EtOH (0.7 mL), and 2 M Na_2CO_3(aq) (1.0 mL) were added under a positive pressure of argon. The mixture was degassed by three freeze-pump-thaw cycles, then stirred at 100 ℃ for 2 d, allowed to cool to rt, diluted with EtOAc (10 mL), and washed with water (10 mL). The organic layer was separated and the aqueous layer was extracted with EtOAc (3×). The organic layers were combined, washed with brine, dried ($MgSO_4$), filtered, and concentrated. The crude product was purified by flash chromatography (2:1 hexanes:CH_2Cl_2) to give 485 mg (80%) of compound **5** as light yellow foam: ^{1}H NMR ($CDCl_3$, 500 MHz, Figure S13) the spectrum is broadened by slow conformational exchange, as would be expected for an *o*-phenylene hexamer with two terminal substituents[11] δ 7.5–4.7 (br, 18H), 4.2–3.0 (br, 14H), 2.0–0.5 (br, 76H); HRMS (ESI) calcd for $C_{78}H_{108}Cl_2NaO_6$ ($M + Na^+$) 1233.7421, found 1233.7385.

Bis(triphenylene) Tp_2

A Schlenk vacuum tube was charged with **5** (606 mg, 0.500 mmol), $PdCl_2(PCy_3)_2$ (146 mg, 0.198 mmol), DBU (152 mg, 0.998 mmol), and Cs_2CO_3 (326 mg, 1.00 mmol), then evacuated and backfilled with argon (3×). NMP (5.0 mL) was added under a positive pressure of Ar, and then the sealed tube was heated at 150 ℃ for 2 d. After cooling to rt, the suspension was diluted with CH_2Cl_2 (10 mL), filtered through Celite, and concentrated. Purification by flash chromatography (3:2 hexanes:CH_2Cl_2) gave 515 mg (90%) of **Tp_2** as an amorphous yellow solid: ^{1}H NMR ($CDCl_3$, 500 MHz, Figure S16) δ 9.26 (m, 2H), 8.46 (d, $\mathcal{J}$ = 9.1 Hz, 2H), 8.36 (d, $\mathcal{J}$ = 9.2 Hz, 2H), 7.96 (s, 2H), 7.28 (dd, $\mathcal{J}$ = 8.9 Hz, $\mathcal{J}$ = 2.6 Hz, 2H), 7.1–7.0 (m, 6H), 4.30 (m, 2H), 4.17 (m, 2H), 4.02 (s, 6H), 2.8–2.6 (m, 4H), 2.2–2.1 (m, 2H), 1.9–1.8 (m, 4H), 1.6–1.5 (m, 2H), 1.5–1.1 (m, 16H), 1.1–0.8 (m, 42H), 0.8–0.7 (m, 2H), 0.7–0.5 (m, 2H), 0.32 (m, 3H), 0.22 (m, 3H); ^{13}C NMR ($CDCl_3$, 125 MHz, Figure S17) δ 157.6, 156.9, 156.1, 136.1, 131.5, 130.9, 130.3, 130.02, 129.99, 129.96, 125.49, 125.46, 124.99, 124.96, 124.2, 123.5, 123.0, 117.8, 115.9, 115.83, 115.77, 111.9, 111.8, 111.2, 110.73, 110.67, 110.6, 68.1, 67.91, 67.89, 65.9, 65.7, 55.5, 39.5, 39.4, 39.14, 39.07, 37.7, 37.64, 37.60, 37.0, 36.8, 35.7, 35.6, 30.41, 30.39, 30.2, 30.1, 29.7, 29.5, 28.2, 28.12, 28.07, 24.9, 24.8, 24.64, 24.61, 24.4, 24.3, 22.9, 22.82, 22.79, 22.75, 22.70, 19.9, 19.8, 19.7, 19.1,

18.7;[b] HRMS (ESI) calcd for $C_{78}H_{106}NaO_6$ ($M + Na^+$) 1161.7887, found 1161.7875.

Tetrabenzanthanthrene TBAA

Compound **Tp$_2$** (11.4 mg, 0.0100 mmol) was dissolved in freshly distilled CH_2Cl_2 (10 mL) and degassed with an Ar stream for 15 min. A solution of $FeCl_3$ (11.4 mg, 0.0703 mmol) in anhydrous CH_3NO_2 (0.3 ml) was added dropwise. Throughout the reaction, a constant stream of Ar was bubbled through the mixture. The reaction was stirred for 30 min and then quenched by adding CH_3OH (15 mL). The mixture was then concentrated, diluted with CH_2Cl_2 (10 mL), filtered through a 3 cm thick pad of Celite, and concentrated again. The crude product was purified by flash chromatography (4:3 hexanes:CH_2Cl_2) to give 6.3 mg (55%) of compound **TBAA** as an amorphous yellow solid: ^{1}H NMR ($CDCl_3$, 500 MHz, Figure S19) δ 9.70 (s, 2H); 9.41 (d, $\mathcal{J}$ = 2.0 Hz, 2H), 8.75 (d, $\mathcal{J}$ = 9.0 Hz, 2H), 8.65 (d, $\mathcal{J}$ = 9.1 Hz, 2H), 7.66 (d, $\mathcal{J}$ = 8.9 Hz, 2H), 7.34 (dd, $\mathcal{J}$ = 8.8 Hz, $\mathcal{J}$ = 2.4 Hz, 2H), 4.5–4.4 (m, 4H), 4.4–4.3 (m, 4H), 4.08 (s, 6H), 2.3–2.2 (m, 2H), 2.2–2.1 (m, 2H), 2.0–1.8 (m, 6H), 1.8–1.7 (m, 2H), 1.6–1.1 (m, 28H), 1.07 (d, $\mathcal{J}$ = 6.2 Hz, 6H), 1.00 (d, $\mathcal{J}$ = 7.2 Hz, 6H), 0.88 (d, $\mathcal{J}$ = 6.5 Hz, 12H), 0.82 (d, $\mathcal{J}$ = 6.6 Hz, 12H); ^{13}C NMR ($CDCl_3$, 125 MHz, Figure S20) δ 157.7, 155.3, 154.4, 130.3, 126.8, 126.7, 125.5, 124.8, 123.94, 123.88, 121.3, 119.8, 118.8, 117.6, 116.2, 112.5, 111.8, 111.7, 68.8, 68.3, 55.6, 39.5, 39.4, 37.9, 37.62, 37.61, 37.4, 37.3, 30.4, 29.9, 28.2, 28.1, 24.9, 22.9, 22.83, 22.76, 22.7, 20.0; HRMS (MALDI) calcd for $C_{78}H_{102}O_6$ (M^+) 1134.768, found 1134.774.

Compound **TBAA′** was obtained as a byproduct as an amorophous greenish-yellow solid (16%): ^{1}H NMR ($CDCl_3$, 500 MHz, S21) δ 10.13 (d, $\mathcal{J}$ = 9.1 Hz, 1H), 9.41 (d, $\mathcal{J}$ = 2.7 Hz, 1H), 9.29 (d, $\mathcal{J}$ = 2.7 Hz, 1H), 8.92 (d, $\mathcal{J}$ = 9.6 Hz, 1H), 8.86 (d, $\mathcal{J}$ = 9.4 Hz, 1H), 8.71 (d, $\mathcal{J}$ = 3.4 Hz, 1H), 8.69 (d, $\mathcal{J}$ = 3.4 Hz, 1H), 8.61 (d, $\mathcal{J}$ = 9.1 Hz, 1H), 8.44 (s, 1H), 7.66 (d, $\mathcal{J}$ = 8.9 Hz, 1H), 7.54 (d, $\mathcal{J}$ = 8.8 Hz, 1H), 7.37 (dd, $\mathcal{J}$ = 8.9 Hz, $\mathcal{J}$ = 2.7 Hz, 1H), 7.31 (dd, $\mathcal{J}$ = 8.9 Hz, $\mathcal{J}$ = 2.7 Hz, 1H), 4.5–4.3 (m, 6H), 4.06 (s, 6H), 2.3–2.1 (m, 3H), 2.0–1.8 (m, 6H), 1.5–1.1 (m, 21H), 1.07 (d, $\mathcal{J}$ = 6.4 Hz, 6H), 1.05 (d, $\mathcal{J}$ = 6.5 Hz, 3H), 0.89 (d, $\mathcal{J}$ = 6.6 Hz, 18H); ^{13}C NMR chemical shifts were extracted from the HMQC (Figure S23) and HMBC (Figure S24)) spectra, see Table S1; HRMS (MALDI) calcd for $C_{68}H_{82}O_5$ (M^+) 978.616, found 978.616.

NMR Spectra

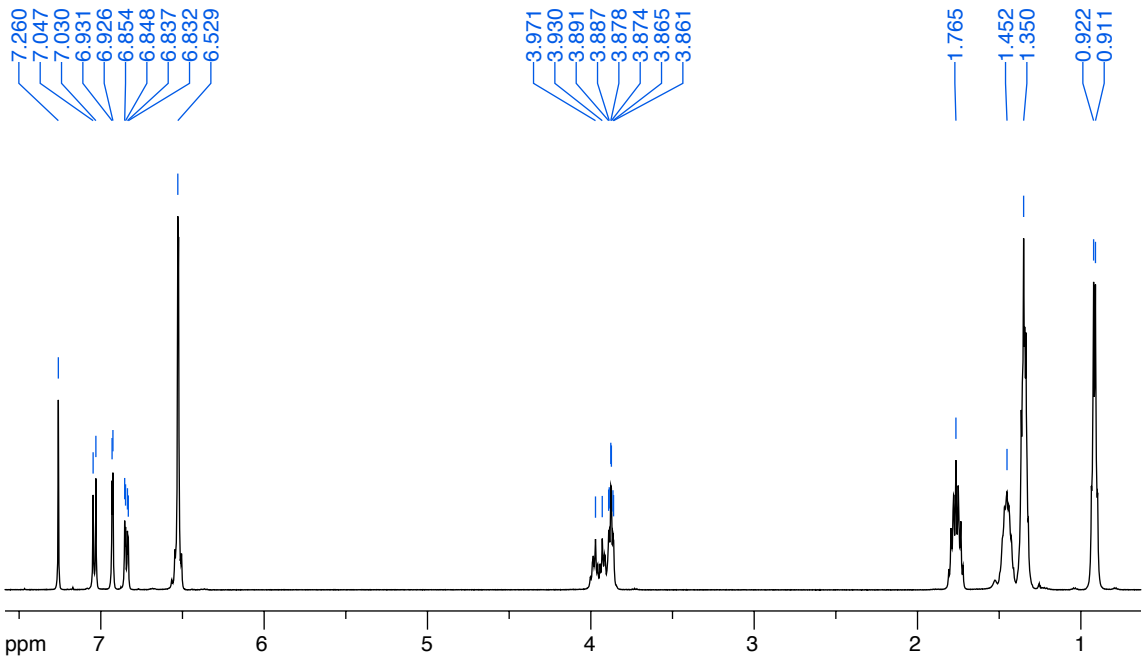

Figure S7. ^{1}H NMR spectrum (500 MHz, $CDCl_3$) of compound **oP^4**.

[b] Although the spectrum is clean, some extra peaks are observed. These peaks appear as clusters, and likely correspond to the different diastereomers resulting from the random configurations of the chiral centers in the 3,7-dimethyloctyloxy side-chains.

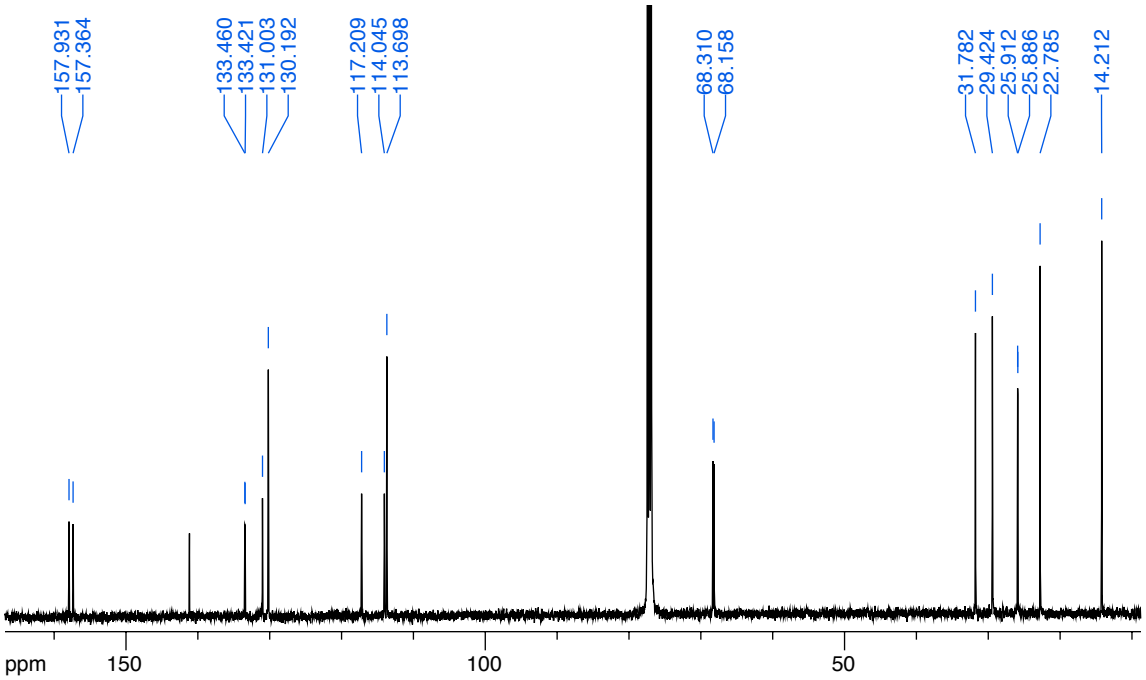

Figure S8. ^{13}C NMR spectrum (125 MHz, $CDCl_3$) of compound **oP**^{4}.

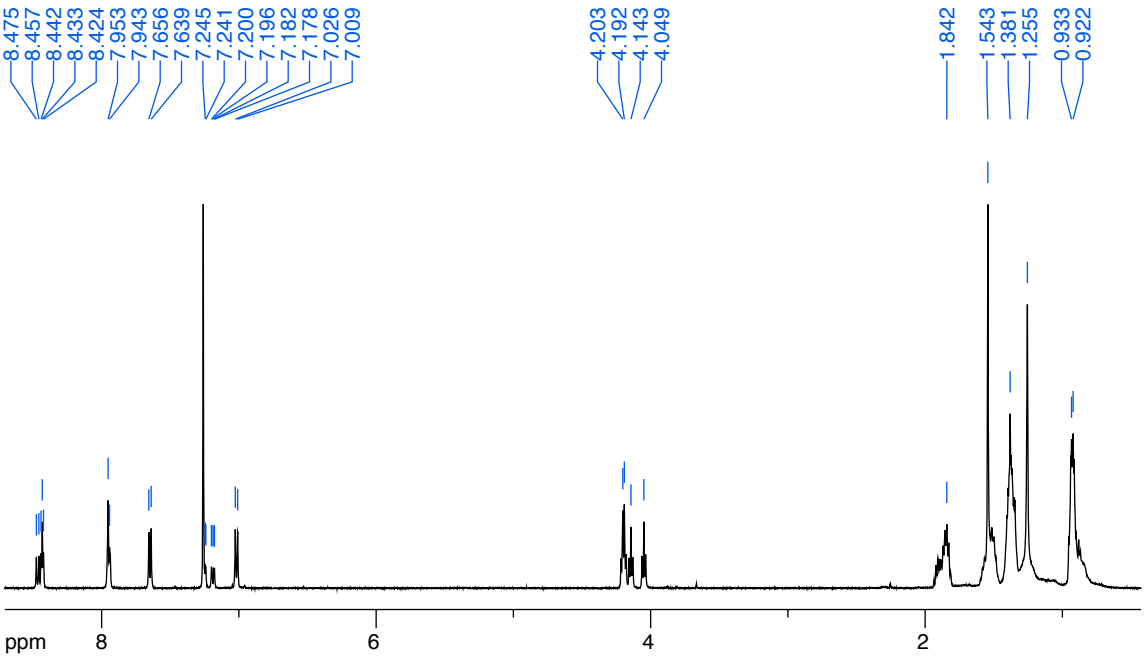

Figure S9. ^1H NMR spectrum (500 MHz, $CDCl_3$) of compound **1**.

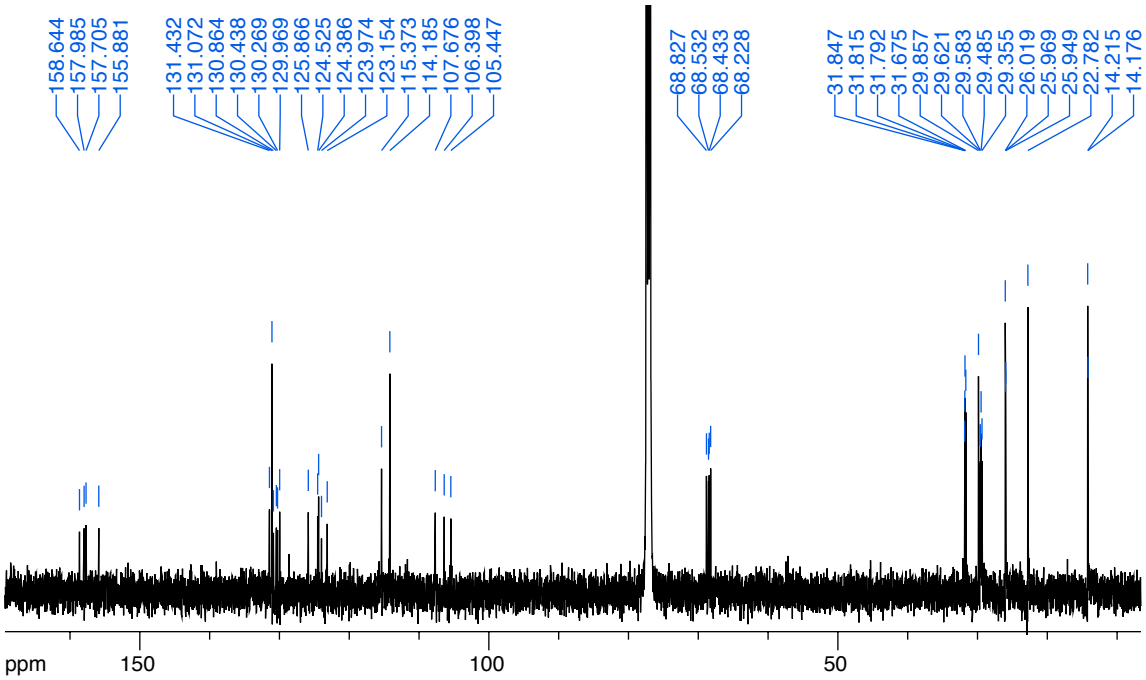

Figure S10. ^{13}C NMR spectrum (125 MHz, $CDCl_3$) of compound **1**.

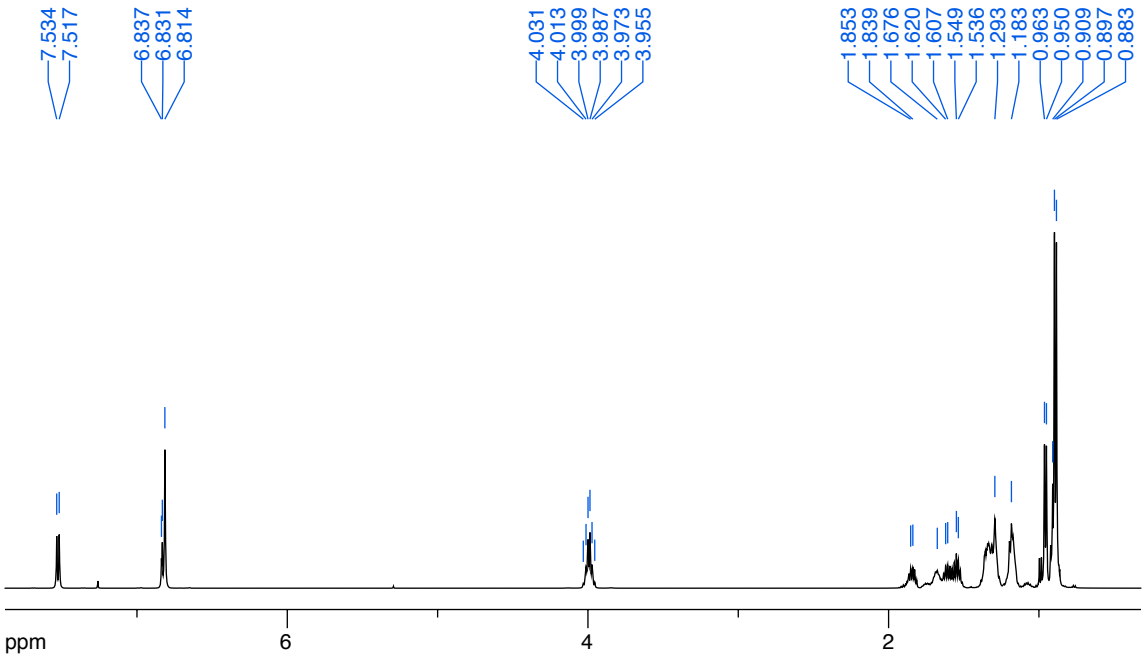

Figure S11. ^{1}H NMR spectrum (500 MHz, $CDCl_3$) of compound **3** (contains some 1-bromo-3,7-dimethyloctane).

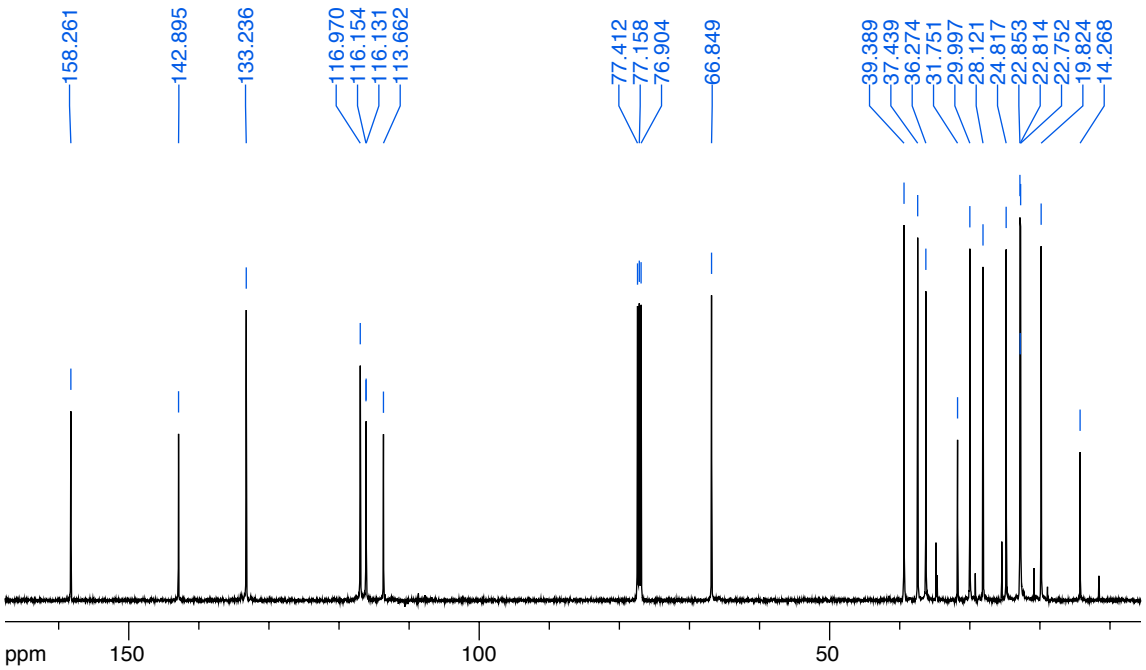

Figure S12. ^{13}C NMR spectrum (125 MHz, $CDCl_3$) of compound **3** (contains some 1-bromo-3,7-dimethyloctane).

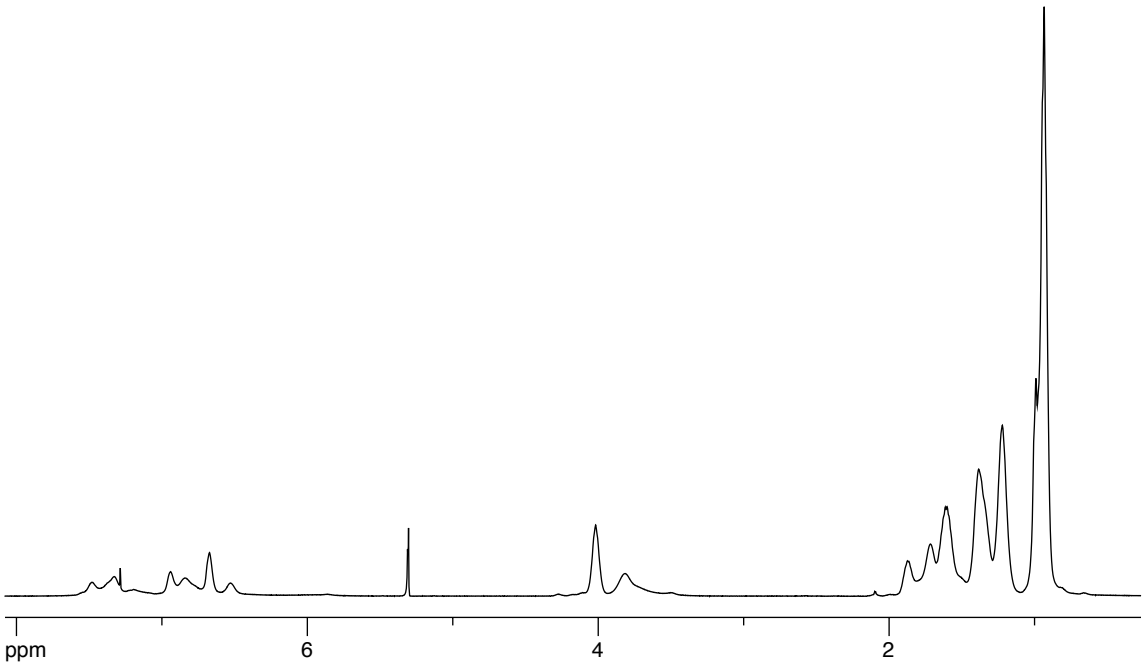

Figure S13. ^{1}H NMR spectrum (500 MHz, $CDCl_3$) of compound **4**.

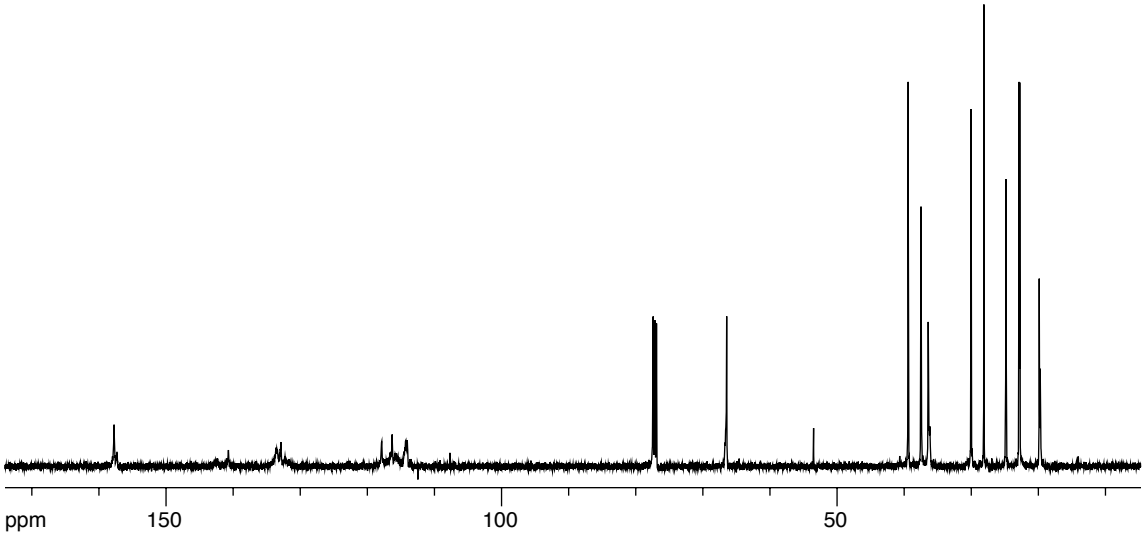

Figure S14. ^{13}C NMR spectrum (125 MHz, $CDCl_3$) of compound **4**

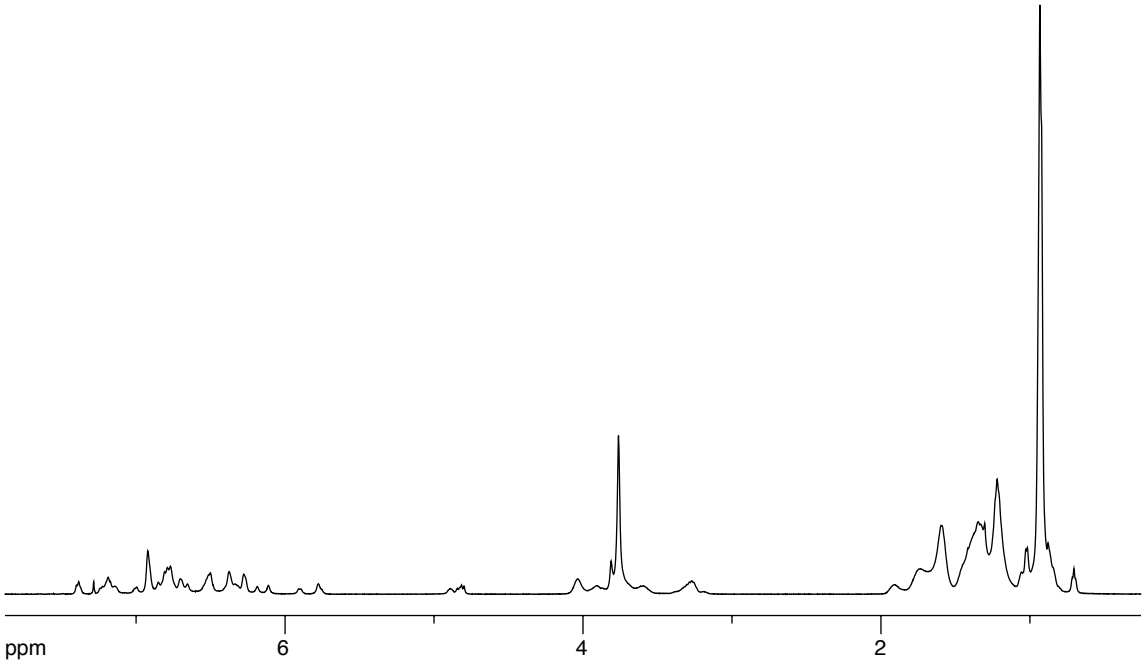

Figure S15. ^{1}H NMR spectrum (500 MHz, $CDCl_3$) of compound **5**.

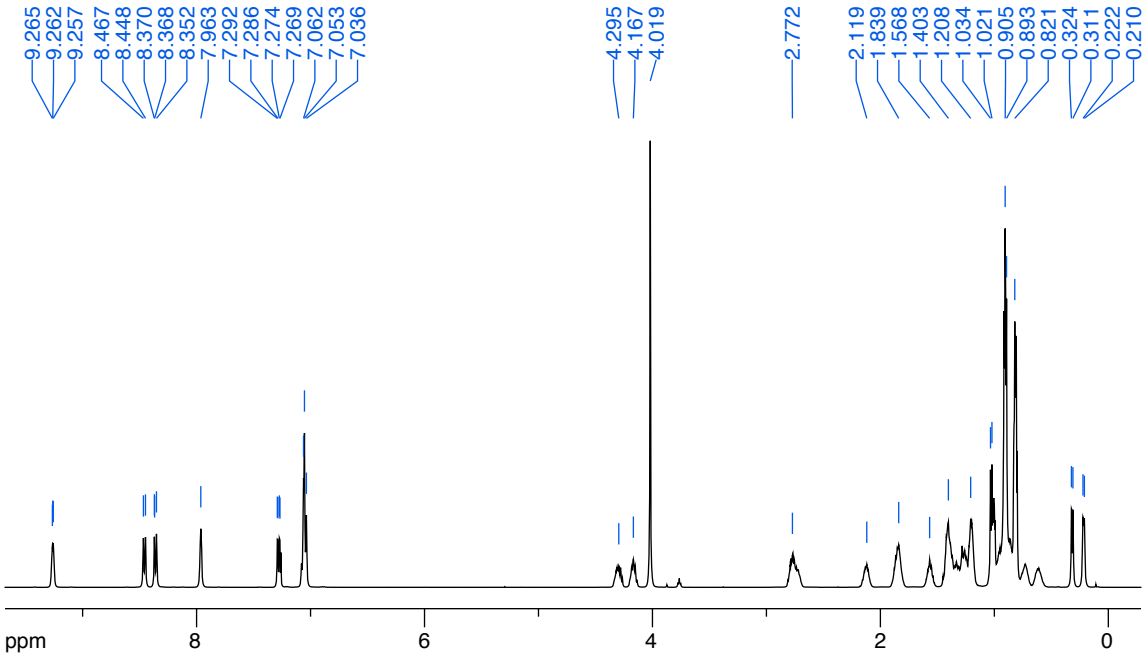

Figure S16. ^{1}H NMR spectrum (500 MHz, $CDCl_3$) of compound **Tp$_2$**.

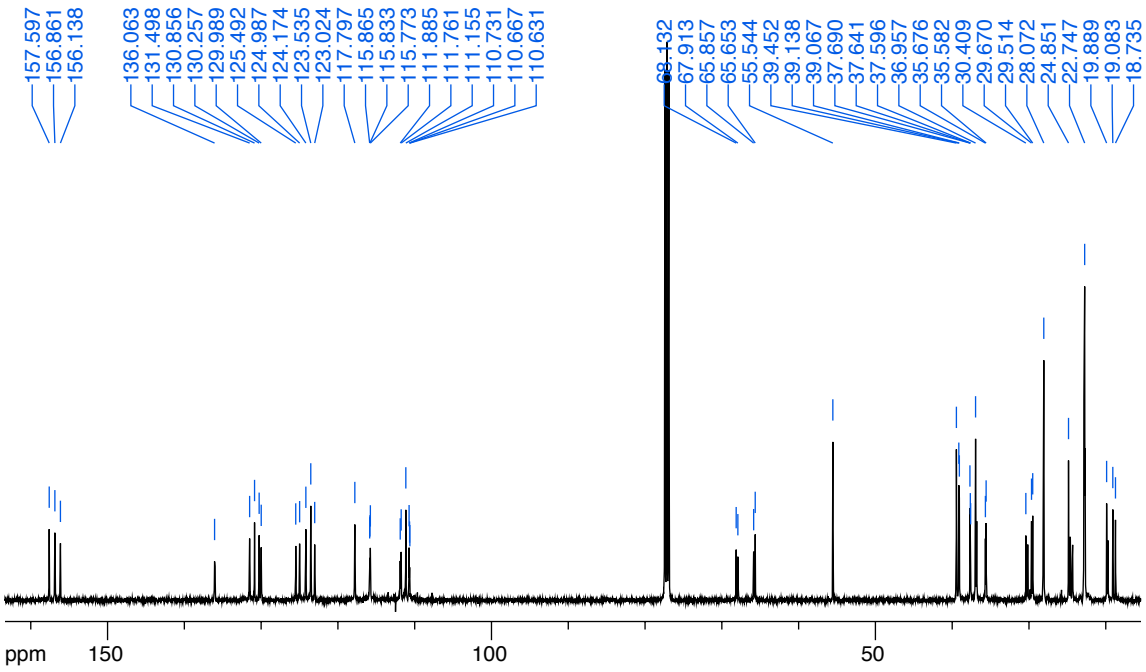

Figure S17. ^{13}C NMR spectrum (125 MHz, $CDCl_3$) of compound **Tp$_2$**

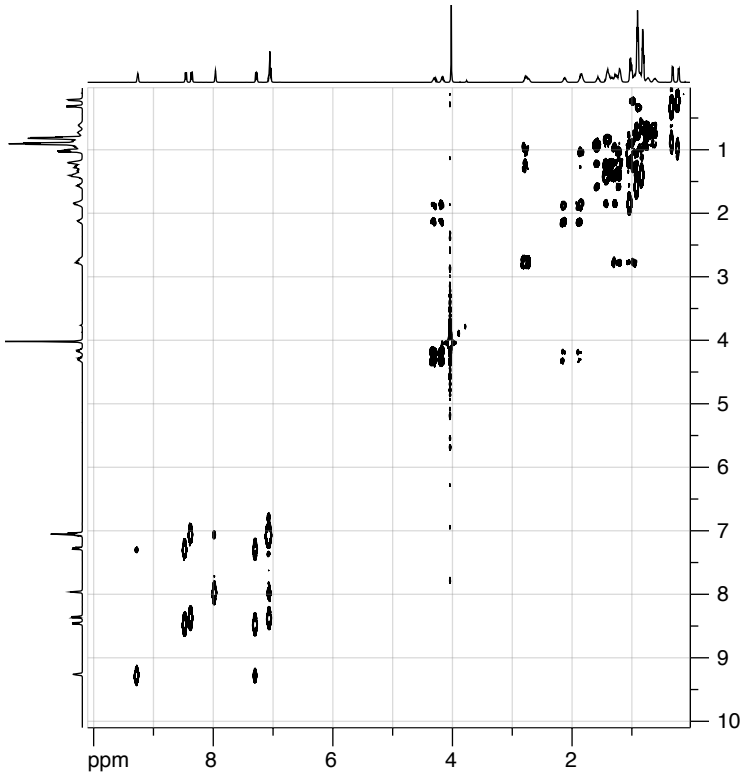

Figure S18. COSY NMR spectrum (500 MHz, $CDCl_3$) of compound **Tp_2**

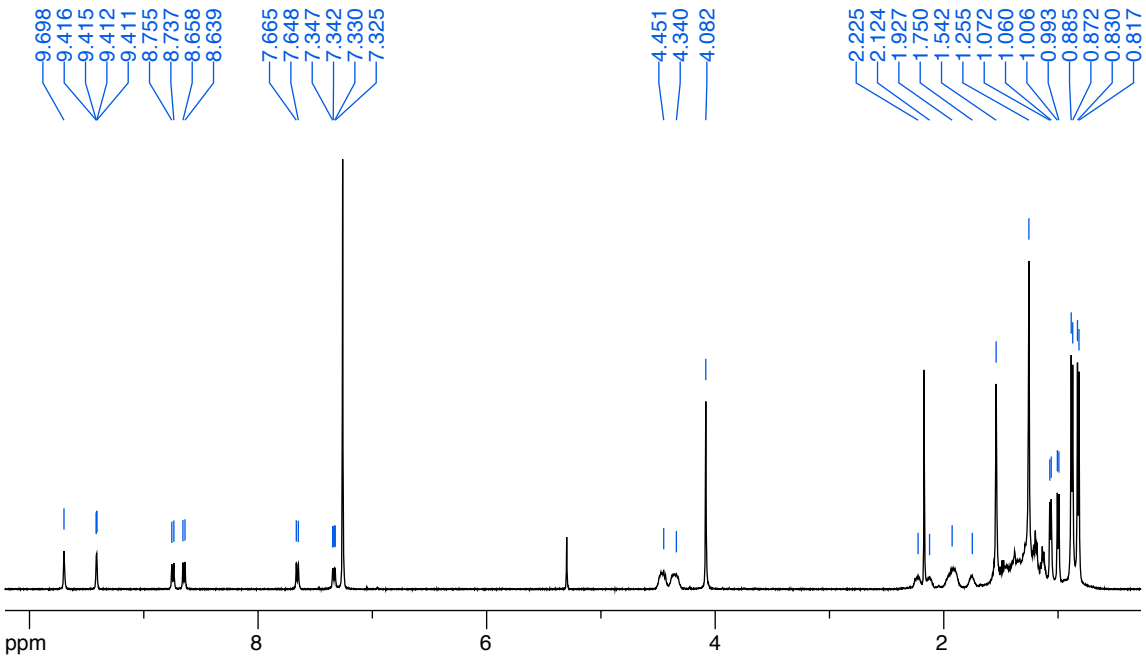

Figure S19. ^1H NMR spectrum (500 MHz, $CDCl_3$) of compound **TBAA**.

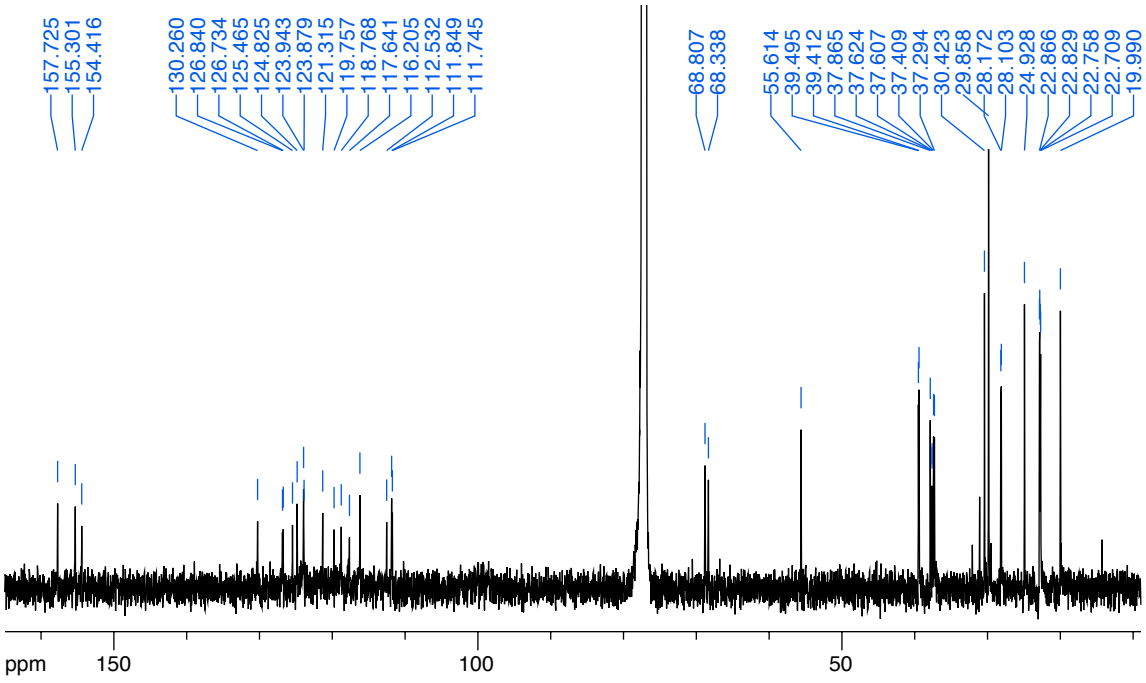

Figure S20. ^{13}C NMR spectrum (125 MHz, $CDCl_3$) of compound **TBAA**

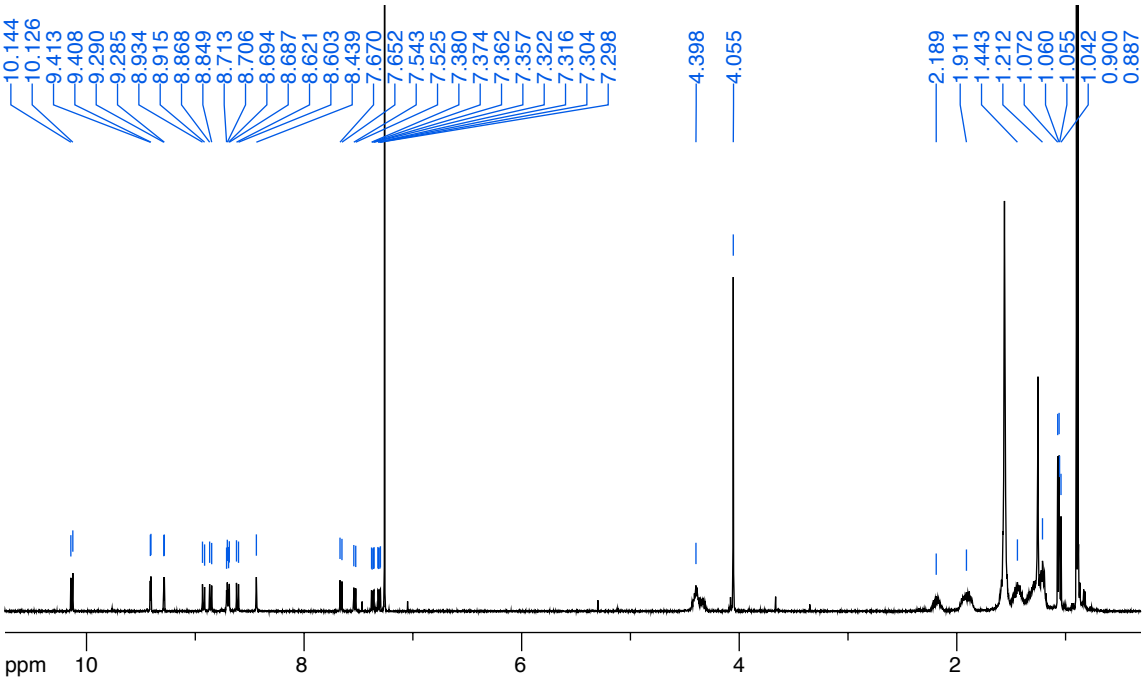

Figure S21. ^{1}H NMR spectrum (500 MHz, $CDCl_3$) of compound **TBAA´**.

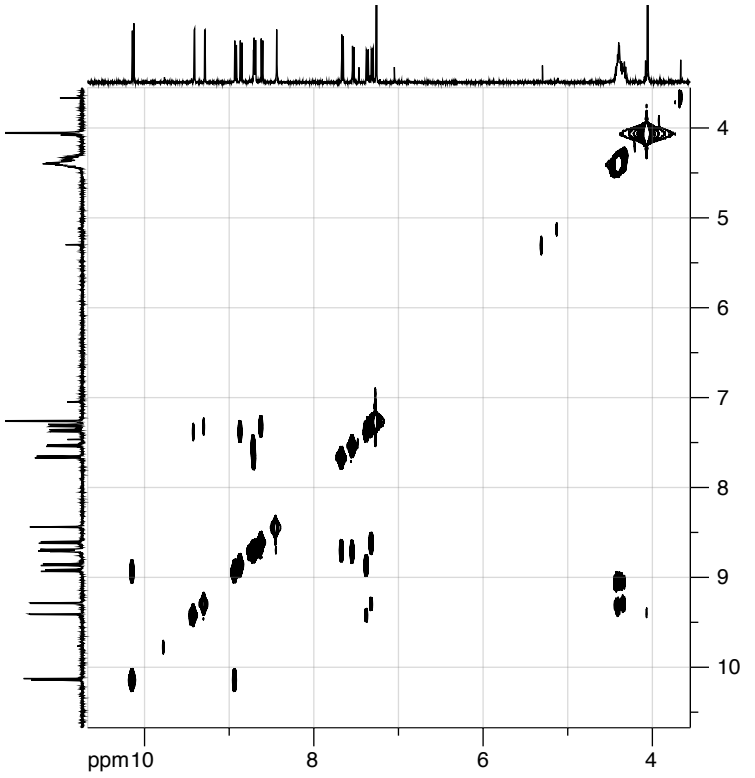

Figure S22. COSY NMR spectrum (500 MHz, $CDCl_3$) of compound **TBAA′**.

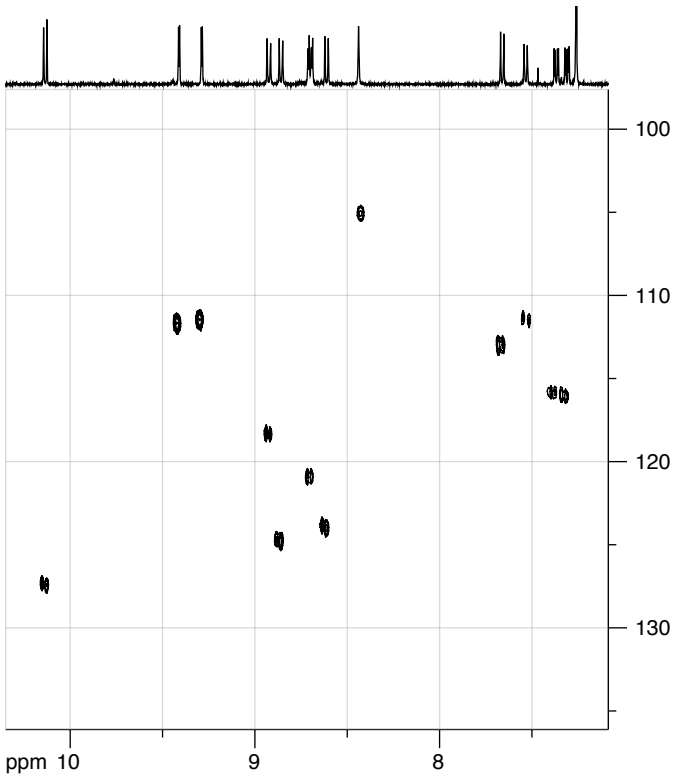

Figure S23. HMQC NMR spectrum (500 MHz, $CDCl_3$) of compound **TBAA′**.

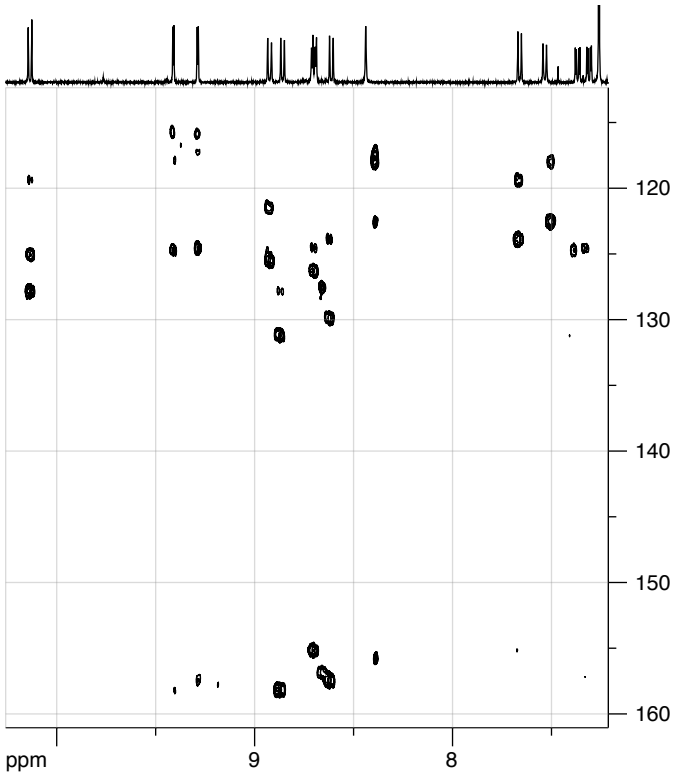

Figure S24. HMBC NMR spectrum (500 MHz, $CDCl_3$) of compound **TBAA′**.

References

(1) M. J. Frisch, G. W. Trucks, H. B. Schlegel, G. E. Scuseria, M. A. Robb, J. R. Cheeseman, G. Scalmani, V. Barone, B. Mennucci, G. A. Petersson, H. Nakatsuji, M. Caricato, X. Li, H. P. Hratchian, A. F. Izmaylov, J. Bloino, G. Zheng, J. L. Sonnenberg, M. Hada, M. Ehara, K. Toyota, R. Fukuda, J. Hasegawa, M. Ishida, T. Nakajima, Y. Honda, O. Kitao, H. Nakai, T. Vreven, J. A. Montgomery, Jr, J. E. Peralta, F. Ogliaro, M. Bearpark, J. J. Heyd, E. Brothers, K. N. Kudin, V. N. Staroverov, T. Keith, R. Kobayashi, J. Normand, K. Raghavachari, A. Rendell, J. C. Burant, S. S. Iyengar, J. Tomasi, M. Cossi, N. Rega, J. M. Millam, M. Klene, J. E. Knox, J. B. Cross, V. Bakken, C. Adamo, J. Jaramillo, R. Gomperts, R. E. Stratmann, O. Yazyev, A. J. Austin, R. Cammi, C. Pomelli, J. W. Ochterski, R. L. Martin, K. Morokuma, V. G. Zakrzewski, G. A. Voth, P. Salvador, J. J. Dannenberg, S. Dapprich, A. D. Daniels, O. Farkas, J. B. Foresman, J. V. Ortiz, J. Cioslowski and D. J. Fox, Gaussian 09*, Rev. B.01*, Gaussian, Inc., Wallingford, CT, 2010.

(2) D. C. Young, *Computational Chemistry*, John Wiley & Sons, Inc., New York, USA, 2001.

(3) A. Ajaz, E. C. McLaughlin, S. L. Skraba, R. Thamatam and R. P. Johnson, *J. Org. Chem.*, 2012, **77**, 9487–9495.

(4) P. Rempala, J. Kroulík and B. T. King, *J. Org. Chem.*, 2006, **71**, 5067–5081.

(5) M. Di Stefano, F. Negri, P. Carbone and K. Müllen, *Chem. Phys.*, 2005, **314**, 85–99.

(6) R. B. Martin, *Chem. Rev.*, 1996, **96**, 3043–3064.

(7) P. R. Mitchell and H. Sigel, *Eur. J. Biochem.*, 1978, **88**, 149–154.

(8) See: http://github.com/scotthartley/NMR_dilution_fit.

(9) S. Mathew, L. A. Crandall, C. J. Ziegler and C. S. Hartley, *J. Am. Chem. Soc.*, 2014, **136**, 16666–16675.

(10) I. Nagao, M. Shimizu and T. Hiyama, *Angew. Chem., Int. Ed.*, 2009, **48**, 7573–7576.

(11) C. S. Hartley and J. He, *J. Org. Chem.*, 2010, **75**, 8627–8636.